HUMAN VACCINES & IMMUNOTHERAPEUTICS
2025, VOL. 21, NO. 1, 2473183
https://doi.org/10.1080/21645515.2025.2473183

Taylor & Francis
Taylor & Francis Group

RESEARCH ARTICLE

OPEN ACCESS Check for updates

The characterization of technical design of a virus-like structure (VLS) nanodelivery system as vaccine candidate against SARS-CoV-2 variants

Jingjing Zhang[a,b*], Fengyuan Zeng[a*], Yanmei Li[a], Changyong Mu[a], Change Liu[a], Lichun Wang[a], Xiaowu Peng[a], Liping He[a], Yanrui Su[a], Hongbing Li[a], An Wang[a], Lin Feng[a], Dongxiu Gao[a], Zhixiao Zhang[a], Gang Xu[a], Yixuan Wang[a], Rong Yue[a], Junbo Si[a], Lichun Zheng[a], Xiong Zhang[a], Fuyun He[a], Hongkun Yi[a], Zhongshu Tang[a], Gaocan Li[a], Kaili Ma[a,b], and Qihan Li[a]

[a]Weirui Biotechnology (Kunming) Co. Ltd, Ciba Biotechnology Innovation Center, Kunming, Yunnan, China; [b]Shandong Weigao Litong Biological Products Co, Ltd, Weihai, China

ABSTRACT

The constant mutation of SARS-CoV-2 has led to the continuous appearance of viral variants and their pandemics and has improved the development of vaccines with a broad spectrum of antigens to curb the spread of the virus. The work described here suggested a novel vaccine with a virus-like structure (VLS) composed of combined mRNA and protein that is capable of stimulating the immune system in a manner similar to that of viral infection. This VLS vaccine is characterized by its ability to specifically target dendritic cells and/or macrophages through S1 protein recognition of the DC-SIGN receptor in cells, which leads to direct mRNA delivery to these innate immune cells for activation of robust immunity with a broad spectrum of neutralizing antibodies and immune protective capacity against variants. Research on its composition characteristics and structural features has suggested its druggability. Compared with the current mRNA vaccine, the VLS vaccine was identified as having no cytotoxicity at its effective application dosage, while the results of safety observations in animals revealed fewer adverse reactions during immunization.

ARTICLE HISTORY
Received 15 January 2025
Revised 11 February 2025
Accepted 24 February 2025

KEYWORDS
Virus-like structure; immunity; mRNA vaccine; dosage

Introduction

Since the pandemic of COVID-19 occurred in Wuhan city and spread rapidly worldwide in 2019,[1] many studies have focused on the development of vaccines, especially the development of mRNA vaccines, which has propelled great progress in this field.[2,3] These works created novel opportunities that enable the realization of a technical strategy in which viral vaccines activate immunity more efficiently through eliciting an intracellular innate immune response followed by adaptive immunity on the basis of molecular biological simulations of viral replication in cells,[4] as mRNA vaccines against COVID-19 have produced great public health effects and business profits.[5] This design of a viral vaccine, which is based on our knowledge of viral molecular biology, involves an artificially unique viral antigenic gene module containing the initiator element (5'-UTR) and terminator element (3'-UTR) with a poly-A tail and can express a certain viral antigen intracellularly, which leads to the binding of these antigenic components to innate immune receptors followed by their activation.[6,7] The realization of this design is dependent on the development of a certain delivery system that works through its fusion effect with the cellular membrane,[4,8] which actually reflects an analogous process of virus entry into cells, even if it is nonspecific to various cells. Importantly, this successful technical design, supported by some licensed and marketed mRNA vaccines,[5] also created a technical concept of a virus-like structure by means of logical consequences. This concept highlights a certain nanodelivery system capable of not only encapsulating mRNA molecules but also loading a protein antigenic molecule on its surface that functions to specifically guide the lipid particle to certain cells, e.g., dendritic cells or other antigen-presenting cells. The significance of this concept includes the following: first, the process by which lipid particles encapsulate mRNAs to target certain cells by loading proteins on their surface to bind to cellular receptors is comparable to that by which viruses bind to cells with membrane proteins to target specific receptors; second, the integration of intracellular antigens encoded by mRNAs and protein antigens loaded on the surface could result in a more extensive antigen spectrum than current mRNA vaccines. If this is the case, this strategy could show a greater advantage for the vaccine development of SARS-CoV-2, which has been haunted for a long time, with waned immunity quickly and lower efficacy against appearing variants of current vaccines.[9,10] On the basis of the above hypothesis, the work described here provides a novel lipid nanodelivery system and suggests a virus-like structure (VLS) vaccine candidate

CONTACT Qihan Li imbcams_qhli@163.com; Kaili Ma mklpumc@gmail.com Weirui Biotechnology (Kunming) Co. Ltd, Ciba Biotechnology Innovation Center, Longquan Road, Kunming, Yunnan 650000, China.
*First Author: Jingjing Zhang (zhangjingjing940115@imbcams.com.cn); Fengyuan Zeng (zengfengyuan0120@163.com).
Supplemental data for this article can be accessed on the publisher's website at https://doi.org/10.1080/21645515.2025.2473183

against SARS-CoV-2 variants. This design of VLS vaccine candidates depends upon the characterization of the lipid nanodelivery system, which has a composition different from that of the current LNP system, and presents critical immunogenicity. The characterization of these lipid components and the properties of the VLS vaccine were investigated to understand their mechanisms.

Materials and methods

Ethics statement

BALB/c mice were purchased from Vital River (Beijing, China) (animal license number: SCXK [Jing] 2021–0006). The experimental mice were specific pathogen-free (SPF) grade and aged 4–5 weeks. The mice were bred in specific pathogen-free (SPF)-grade barrier facilities [laboratory license number: SYXK (Dian) K2023–0010]. The laboratory animals were cared for and used according to the "3 Rs" principle and animal welfare guidelines. The animal experimental process and animal-related care and welfare were reviewed and approved by the Animal Experiment Ethics Committee of Shandong WeigaoLitong Biological Products Co., Ltd. (approval number: LACUC- RD3-2022-006).

Cell lines

HEK-293T cells and 16HBE cells (ATCC, Manassas, Virginia, USA) were cultured in Dulbecco's modified Eagle's medium (DMEM, Thermo Fisher Scientific, Waltham, Massachusetts, USA) supplemented with 10% fetal bovine serum (FBS; HyClone, GE Healthcare, Chicago, Illinois, USA), 10% 100 U/ml penicillin and 100 mg/ml streptomycin. JASWII dendritic cells (ATCC, Manassas, Virginia, USA) were cultured in MEM Alpha (Thermo Fisher Scientific, Waltham, Massachusetts, USA) supplemented with 20% fetal bovine serum (FBS; HyClone, GE Healthcare, Chicago, Illinois, USA), 10% 100 U/ml penicillin, 100 mg/ml streptomycin, and 5 ng/ml murine GM-CSF (HY-P7361, MCE, USA).

Animal experimental design

BALB/c mice were divided into seven groups, namely, the control group and the other six immunized groups, depending on the N/P ratio. The six groups were vaccinated with VLS at different dosages, and the VLS contained 15/20/25 μg of mRNA and 5/7.5/10 μg of protein. All the mice in the immunized groups underwent booster immunization on the 21st day after the primary immunization and on the 14th day after the booster immunization for antibody detection.

To compare the immunity of the three types of vaccines, BALB/c mice were randomly divided into four groups: the VLS group ($n = 20$), the ADT-LNP-mRNA group ($n = 20$), the ADT-LNP-protein group ($n = 20$) and the control group. The VLS contained 20 μg of mRNA and 5 μg of protein, and the ADT-LNP-mRNA and ADT-LNP-protein contained only 20 μg of mRNA or 5 μg of protein. All the mice in the immunized groups underwent booster immunization on the 21st day after the primary immunization and 28 days after the booster immunization for antibody detection.

Cytotoxicity assay

HEK-293T cells were seeded at a density of 5×10^4 mL^{-1} in 96-well plates and incubated at 37°C with 5% CO_2 for 24 h. The cells were treated with the VLS vaccine and cultured for another 24 h. Cell proliferation rates were subsequently assessed via a cell counting kit-8 (CCK-8) assay (Biosharp, BS350B, China) according to the manufacturer's instructions.

Cell transfection

LNP-mRNA and the VLS vaccine were transfected into 293T cells, 16HBE cells, and JASWII DCs, and Western blot analysis was performed at 24 h after transfection.

Western blotting

Proteins were separated on 4–20% SDS – PAGE gels (M42015C, GenScript Biotech, China) and transferred to polyvinylidene difluoride (PVDF) membranes. The membranes were blocked with 5% BSA-TBST (Sigma – Aldrich, St. Louis, MO, USA). The membranes were subsequently incubated with an anti-SARS-CoV-2 S1 antibody (MHC0102; Yunnan Lepeng Technology Co., Ltd.) for 12 h at 4°C, washed 3 times with TBST for 5 min each, incubated with HRP-conjugated goat anti-mouse IgG (H + L) (Sigma, Shanghai, China) for 1 h at room temperature, and washed 3 times with TBST for 5 min each. Finally, the PVDF membranes were covered with ECL ultrasensitive chemiluminescence reagent (NCM Biotech, Cat# P10100, Suzhou, China) and placed in a Bio-Rad gel imager for exposure and color development.

Hemolysis test

Mouse blood was centrifuged at 1500 rpm for 10 min, the supernatant was discarded, and the erythrocytes were washed by adding 5–8 ml of PBS (pH 7.2) and centrifuging at 1500 rpm three times for 10 min. The volume of red blood cells was measured, and a 5% red blood cell suspension was diluted in PBS (pH 7.2) and stored at 4°C. The samples were diluted according to the gradient and subsequently added to the plate. After the sample was added, the volume was adjusted to 500 μl added 500 μl of the 5% red blood cell suspension in PBS (pH 7.2). The positive control was 500 μl of 0.5% Triton-X-100 added 500 μl of the 5% red blood cell suspension. Five hundred microliters of PBS added 500 μl of the 5% red blood cell suspension were incubated for 1 h at 37°C and centrifuged for 5 min at 1500 rpm, after which the supernatant was removed, 100 μl/well was added to the microplate, and the OD540 was read.

Design and preparation of different lipid nanoparticles

Briefly, five compositions were prepared by encapsulating equivalent amounts (20 μg) of mRNA to explore the interactions of mRNAs and proteins with different cationic lipid molecules. The five compositions were prepared by mixing the different

components of NanoAssemblr® Ignite+™ LNPs (Precision Nanosystems, Canada) according to Table 2 with mRNA at a weight ratio of 1:3 in 20 mm NaAc, 2.5 mm KCl and 0.1% trehalose buffer.

Furthermore, different S1 proteins (His or His-Free) were added to the five compositions at concentrations of 0.1, 0.5, 1, and 5 μg/500 μl to test the protein binding ratio.

Flow NanoAnalyzer

The use of the Flow NanoAnalyzer has been described elsewhere. Briefly, SARS-CoV-2 spike protein S1 antibodies were labeled with Alexa Fluor 647 (Abcam). The five components were labeled with the S1 antibody at 37°C for 30 min to determine the protein binding ratio. A nucleic acid dye (SYTO 9, NanoFCM) was added to the lipids, which were subsequently incubated for 15 min at 37°C to determine the ratio of the five components loaded with mRNA.

ELISA

The S1 antibody was measured via ELISA. The absorbance at 450 nm was measured via an ELISA plate reader (Gene Company, Beijing, China). The antibody serum samples that yielded OD values at least 2.1-fold greater than those of the negative control were considered positive. The endpoint titer (ET) was defined as the highest serum dilution that yielded a positive OD value. The geometric mean titer (GMT) was calculated as the geometric mean of the ETs of the positive serum samples in each group.

Statistical analysis

All the data are presented as the mean values with the standard errors of the means. Significant differences between groups were analyzed via t tests (GraphPad Prism; GraphPad Software, San Diego, CA, USA), and $P < 0.05$ was considered to indicate statistical significance.

Results

Theoretical advantages of the VLS nanodelivery system and its limited effect on the currently used LNP system

Previous data concerning the utilization of SARS-CoV-2 mRNA vaccines with mRNA molecules encoding the S or S1 gene confirmed that the lipid particles of the vaccine enabled the delivery of mRNA molecules to various cells of local tissue through LNP fusion to the cellular membrane.[11] This technical breakthrough realized the endogenous expression of vaccine antigens, which is important for increasing the immunogenicity of COVID-19 vaccines, as two points need to be addressed. One is the nonspecificity of LNP fusion to the cellular membrane, which might lead to a lack of targeting specificity and unnecessary damage to some cells. The other is the limited antigenic capacity resulting from the expression of a single mRNA encoding the S antigen, which is unable to prevent the emergence of more variants. The VLS system improves these two inadequacies. First, the S1 protein of SARS-CoV-2 recognizes not only the ACE2 receptor but also the DC-SIGN receptor, which is expressed in immune cells, especially dendritic cells and macrophages.[12,13] These findings suggest that the S1 protein loaded on the surface of the VLS vaccine can guide lipid particle-encapsulated mRNAs to direct dendritic cells/macrophages in the early period of immunization and enhance antigenic signal stimulation and the activation of these antigen-presenting cells. Second, the integration of the endogenous S1 antigen encoded by mRNA and the exogenous S1 protein antigen can expand the antigenic spectrum to address more epitopes of viral variants in vaccines (Supplemental Figure S1). These hypothesized events are shown in Figure 1a. However, our experiment using the

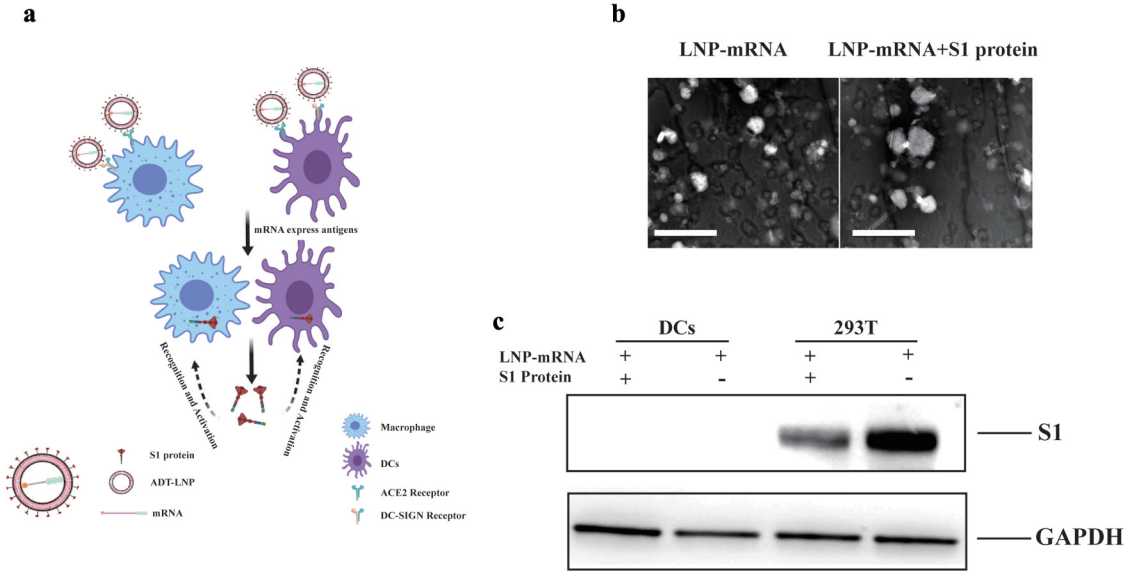

Figure 1. Biological characteristics of the VLS nanodelivery system. (a) The speculated mechanism of VLS vaccines, VLS vaccines are endocytosed by DCs and macrophages through the mediation of S1 protein binding specifically with dc-sign or ACE2 receptor. The delivered mRNA is translated into protein as an endogenous antigen that can activate DCs and macrophages. (b) Electron micrographs of current LNP system and loaded protein. Samples were negatively stained with 2% uranyl acetate (pH 7.4). Scale bars = 200 nm. (c) S1 proteins were expressed by Western blotting analysis of current LNP system or loaded protein.

current LNP system did not support this concept because the accession of the S1 protein antigen enables the alteration of the LNP structure. The results of physicochemical detection suggested that the addition of protein significantly increased the diameter of the LNPs, decreased the zeta potential and altered the shape of the lipid particles (Table 1; Figure 1b). Importantly, the expression of mRNA in 293 cells was decreased, but its expression was not detected in dendritic cells (Figure 1c). These data suggest that the current mRNA vaccine modality cannot be applied according to our VLS hypothesis, even if it possesses attractive technical prospects.

A novel composition of lipid molecules enables the formation of a virus-like structure associated with mRNA genes and protein antigens

Studies on the interactions between lipid molecules and mRNAs in COVID-19 vaccines have suggested that the binding of the positive charge in the head group of ionizable cationic lipids to the negative charge in mRNA molecules supports the encapsulation of mRNAs by LNPs.[14,15] In association with other lipid molecules, including cholesterol, LNP-encapsulated mRNAs present a core–shell model that is composed of an amorphous isotropic core and a surface layer. The structure was found to contain 24% water, except the mRNA and lipid molecules used for analysis.[16] This leads to the possibility that the interaction of mRNA and ionizable cations, both of which are hydrophobic molecules, is likely subject to the existence of water molecules through electrostatic attraction and hydrogen bonding. Generally, this hydration might involve the presence of cholesterol, which has been shown to increase the rigidity of the lipid membrane and probably maintain water molecules during the production of lipid particles. These findings suggest that the mechanism of our observation of current LNPs is that they are unable to carry proteins simultaneously, such as their encapsulated mRNAs. On the basis of these data and previous studies, which involved the interaction of the protein and lipid molecules DOTAP,[17] a novel design composed of two ionizable cation lipid molecules DOTAP and DHA-1, the neutral phospholipids DOPC and mPEG DTA-1-2-K, but free of cholesterol, was suggested for VLS carriers named ADT-LNP. To investigate the roles of each ionizable cation in this structure, five compositions were prepared by encapsulating equivalent amounts of mRNA (Table 2) and interacting with equal amounts of S1 protein, followed by detection with a flow nanoanalyzer. The results suggest two points. First, DHA-1 was identified as being responsible for binding with mRNAs (Figure 2a); it interacted with the same amount of mRNAs in compositions A1, A2 and A3, with a constant molar ratio in these three compositions; however, the composition C was unable to bind mRNAs, which did not contain DHA-1 (Table 2; Figure 2a). Second, DOTAP was identified as being responsible for binding protein (Figure 2b), which was supported by the significant relationship of its decreasing molar ratio and reduced binding protein amount in the A1 to A3 compositions (Table 2; Figure 2b) and higher bound protein amount in the C composition and no protein bound in the B composition (Table 2; Figure 2b). In further morphological detection of the ADT-LNP-mRNA structure produced from the five compositions and those loaded with the S1 protein, A1, A2 and A3 exhibited a regular spherical appearance with a diameter of approximately 100 nm (Figure 2c; Supplemental Table S1). A1 to 3 presented a certain sphere with the small protrusion on its surface (Figure 2d). These data suggest that our design of ADT-LNP enables the realization of the VLS hypothesis.

Analysis of the optimized composition of mRNA and protein in the VLS system

Several licensed mRNA vaccines against SARS-CoV-2 provide different amounts of mRNA (30–100 μg) for realizing effective immunization.[8,18,19] Importantly, however, the validity of the mRNA vaccine was determined not only by the amount of mRNA used but also by the effective integration rate of mRNAs and LNPs,[20] which led to a parameter N/P ratio. In our VLS system, this N/P ratio was investigated to characterize the ability of ADT-LNP to bind mRNA and protein simultaneously. First, we prepared six ADT-LNP-mRNAs with different N/P ratios on the basis of different amounts of mRNA and loaded the same amount of S1 protein on them (Table 3). The analysis of their physicochemical properties suggested that the VLS produced with an N/P ratio of 6–8, which was referenced by current mRNA vaccines, had an obviously lower encapsulating rate of mRNA and loading rate of protein than those produced with a higher N/P ratio (Table 3). Second, on the basis of the N/P ratio from 16–19, the VLS encapsulated and loaded with different amounts of mRNA and protein S1

Table 1. The physicochemical characteristics of classical LNP lipid particles.

	Size (nm)	PDI	Zeta (mV)
LNP-mRNA	120–150	<0.2	12.3 ± 0.012
LNP-mRNA +S1 protein	200–220	<0.2	7.8 ± 0.2

Table 2. Composition of the five lipid particles used to investigate protein/mRNA ratios and cationic lipids (molar ratios).

Sample name	DHA-1	DOTAP	DOPC	mPEG
A1	37.61	5.61	18.70	1.00
A2	37.61	7.01	18.70	1.00
A3	37.61	8.42	18.70	1.00
B	37.61	0.00	18.70	1.00
C	0	8.42	0	0

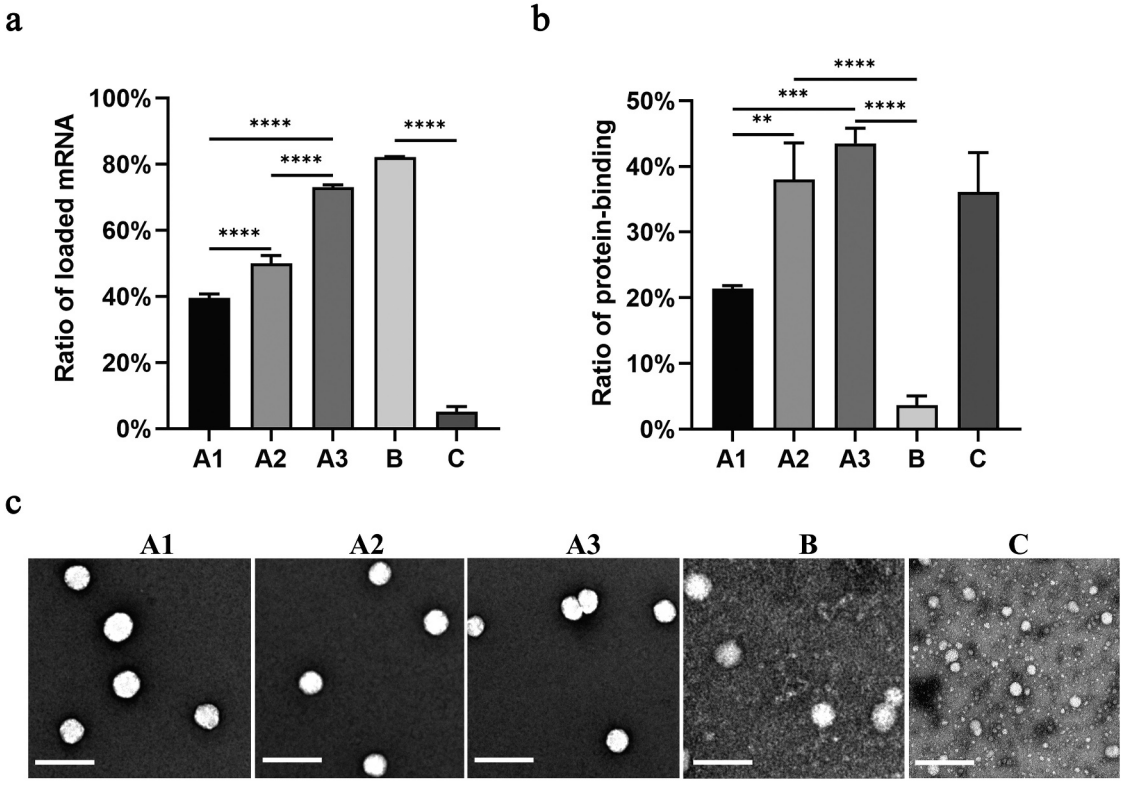

Figure 2. The function and physical characteristics of the five lipid particles. The ratio of loaded mRNA (a) and protein (b) by flow nanoanalyzer; (c) Electron micrographs of A1, A2, A3, B and C. Samples were negatively stained with 2% uranyl acetate (pH 7.4). Scale bars = 200 nm. The data are shown as the means ± SEMs from three independent experiments ($n = 3$); *$P < 0.05$, **$P < 0.01$, ***$P < 0.001$, **** $P < 0.0001$.

Table 3. The physicochemical characteristics of lipid particles with different N/P ratios.

N/P ratios	mRNA (μg/dose)	Protein (μg/dose)	mRNA encapsulated ratio (%)	Protein loaded ratio (%)
6	20	5	89	52.5
7	20	5	85	39.6
8	20	5	87	63.6
17.2	20	5	95	85
19.4	20	5	95	86.2
25.8	20	5	95	84.7

elicited an antibody response that was not significantly different (Table 4). These data suggested an optimized combination of mRNA and protein in the VLS system with a specific N/P ratio of 16–18, which might elicit effective immunity with lower amounts of mRNA and protein. An improved immune-precipitation method identified the specific VLS structure of the system.[11]

Dynamic expression of VLS mRNA in various cells via the S1 protein recognition of ACE2 and DC-SIGN

The critical technical innovation of VLS design focused on the S1 protein loaded on the surface of ADT-LNP-mRNA particles, which enables the recognition of ACE2 and DC-SIGN receptors, which are usually located in dendritic cells and macrophages. This led logically to the process of VLS binding specifically to these cells and delivering mRNA to them, followed by the activation of innate and harvest immunity. To evaluate this mechanism, our experiment included 293 cells, which are usually transfected to detect mRNA expression, but without ACE2 receptors, 16-HBE cells, which are bronchial epithelial cells with ACE2 receptors, and the mouse dendritic cell JASWII strain, which has similar human DC-SIGN receptors but no ACE2,[11] were used to analyze the dynamic expression of ADT-LNP-mRNA and mRNAs used in VLS vaccines at different doses at different times. The results suggested that, first, the same dynamic expression trends of mRNAs in a dose-dependent manner were observed in 293 cells treated with ADT-LNP-mRNA or VLS vaccines (Figure 3a), which were identified via WB (Figure 3a). Second, similar trends in expression in terms of dose effects were found in 16-HBE cells (Figure 3b), but differences in trends were detected in the cells treated with ADT-LNP-mRNA and VLS (Figure 3b), which reflected some differences associated with the existence of ACE2 receptors. Third, completely different trends in mRNA expression were observed in the dendritic cells; only a greater amount of mRNA in the ADT-LNP-mRNA group was found slightly expressed in the dendritic cells rather than lower amount of mRNA (Figure 3c), but a lower amount of mRNA in the VLS vaccine group was capable of expression

Table 4. Antibody titers of animals immunized with lipid particles at different N/P ratios.

N/P ratio	mRNA (μg/dose)	Protein (μg/dose)	immunocompetence	
			primary immunization (D21)	booster immunization (D14)
51.7	15	5	51200–204800	1638400–6553600
	20	7.5	51200–409600	1638400–13107200
	25	10	51200–204800	3276800–6553600
31	15	5	102400–409600	1638400–13107200
	20	7.5	102400–204800	1638400–13107200
	25	10	51200–409600	1638400–13107200
25.8	15	5	51200–204800	1638400–6553600
	20	7.5	102400–409600	1638400–13107200
	25	10	51200–204800	1638400–3276800
19.4	15	5	51200–409600	1638400–13107200
	20	7.5	51200–409600	3276800–13107200
	25	10	51200–409600	1638400–13107200
17.2	15	5	51200–409600	1638400–13107200
	20	7.5	51200–409600	3276800–13107200
	25	10	51200–409600	1638400–13107200
15.5	15	5	51200–409600	1638400–13107200
	20	7.5	51200–409600	1638400–13107200
	25	10	102400–409600	1638400–13107200
8	15	5	51200–204800	819200–6553600
	20	7.5	51200–204800	819200–6553600
	25	10	51200–409600	819200–6553600
7	15	5	25600–204800	819200–6553600
	20	7.5	51200–204800	819200–6553600
	25	10	51200–409600	819200–6553600
6	15	5	25600–102400	819200–6553600
	20	7.5	51200–204800	819200–6553600
	25	10	51200–409600	819200–6553600

clearly in the cells, and a dose-dependent effect on expression was also observed in the VLS group (Figure 3c).[11] The expression of the mRNA in VLS systems in dendritic cells confirmed our design and identified the role of the S1 protein in the VLS system. To further identify the advantages of the VLS over the current mRNA vaccine, ADT-LNP-mRNA and VLS with different amounts of mRNA were used to immunize BALB/c mice. The detection of anti-S antibodies suggested that the VLS group presented a greater dynamic antibody response than did the ADT-LNP-mRNA group (Figure 3d).

VLS vaccine candidates enable broad-spectrum antibody responses against SARS-CoV-2 variants

In our design of the VLS, two purposes were planned: one was to significantly enhance antigenic signal stimulation to elicit robust immunity via the VLS interacting directly with dendritic cells/macrophages, followed by mRNA expression. The other was to extend the antigenic spectrum against SARS-CoV-2 variants on the basis of two units of antigenic capacity, including the S1 antigen encoded by mRNA and protein S1 and a strategy of cross complementation of antigenic epitopes in these two units (Supplemental Figure S1). To evaluate these effects, we established three groups of immunized animals, namely, the VLS group, ADT-LNP-mRNA group and ADT-LNP-protein group (Table 5). Antibody detection via ELISA at 28 days after two immunizations at 0 and 21 days suggested higher antibody titers against variants of WT, Beta, Delta and Omicron in the VLS groups than in the other two groups did (Figure 4a), whereas similar increasing trends of antibody titers against recent variants of XBB.1.5, EG.5.1, JN.1 and KP.2 were detected in the VLS group (Figure 4b). Importantly, further detection of pseudoviruses suggested that these immune sera presented neutralizing antibodies with protective significance (Figure 4c). The real virus neutralization test indicated that the significant neutralizing antibody titers observed against XBB.1.5, JN.1 and KP.2 were the same as those against past variants (Figure 4d). These data suggested that our VLS vaccine achieved primary purposes.

Safety evaluation of VLS vaccine candidates in vitro and in vivo

The safety of the VLS system, a novel nanodelivery system with different compositions versus current LNPs, should be considered because of its validity. In our work, some basic toxicological measurements were performed, except the conventional toxicological research using animals required by authorities. First, on the basis of a previous report that DOTAP can induce hemolysis in red blood cells[21] 31), *in vitro* analysis using DHA-1/DOPC, DOTAP and VLS systems to treat red blood cells indicated that DOTAP led to hemolysis in a dose-dependent manner, similar to its use alone (Figure 5a), and that DHA-1/DOPC did not have this effect (Figure 5b). However, this characterization of hemolysis basically disappeared because of its integration into the ADT-LNP-mRNA system (Figure 5c). Furthermore, the VLS end product containing DOTAP did not completely elicit hemolysis, even at higher doses than those used (Figure 5d). In the animal study, the mice injected with 5× VLS did not exhibit any manifestations or pathological changes in physiological hemolysis (Table 6). In addition, the detection of the cytotoxicity of VLS in CCK-8 cells suggested that only slight toxicological effects were observed (Figure 5e). All of the data, including those provided by the authorized professional toxicological institute, indicated the safety of VLS vaccines, at least in experimental animals.

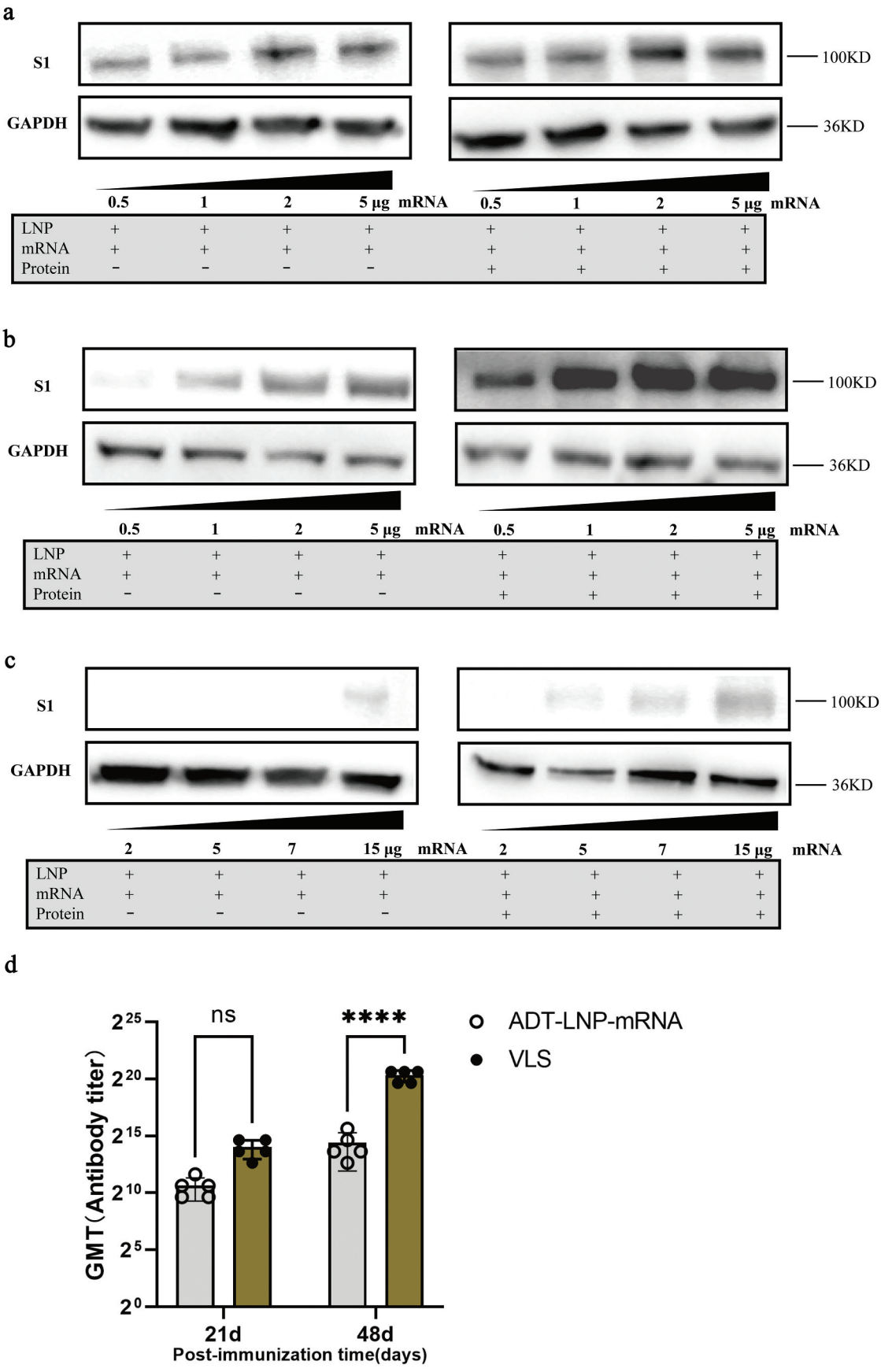

Figure 3. Different dynamic expression patterns of the VLS in 293, 16HBE and dendritic cells are based on the interaction of the S1 protein. S1 proteins were expressed by Western blotting analysis of 293T cells (a), 16HBE cells (b) and dendritic cells (c) transfected with ADT-LNP-mRNA or VLSs containing different doses (0.5, 1, 2, 5, 7, 15 μg) of S1 mRNA for 48 h. (d) SARS-CoV-2 titers of specific Anti-Omicron strain antibodies whose production was induced by ADT-LNP-mRNA or VLSs, the hollow circles represent the ADT-LNP-mRNA and solid circles represent the VLS. The data are shown as the means ± SEMs from three independent experiments ($n = 5$). *$P < 0.05$, **$P < 0.01$, ***$P < 0.001$, ****$P < 0.0001$.

Table 5. Groups of immunized animals.

Group	mRNA (μg/dose)	Protein (μg/dose)
VLS	20	5
ADT-LNP-mRNA	20	0
ADT-LNP-Protein	0	5

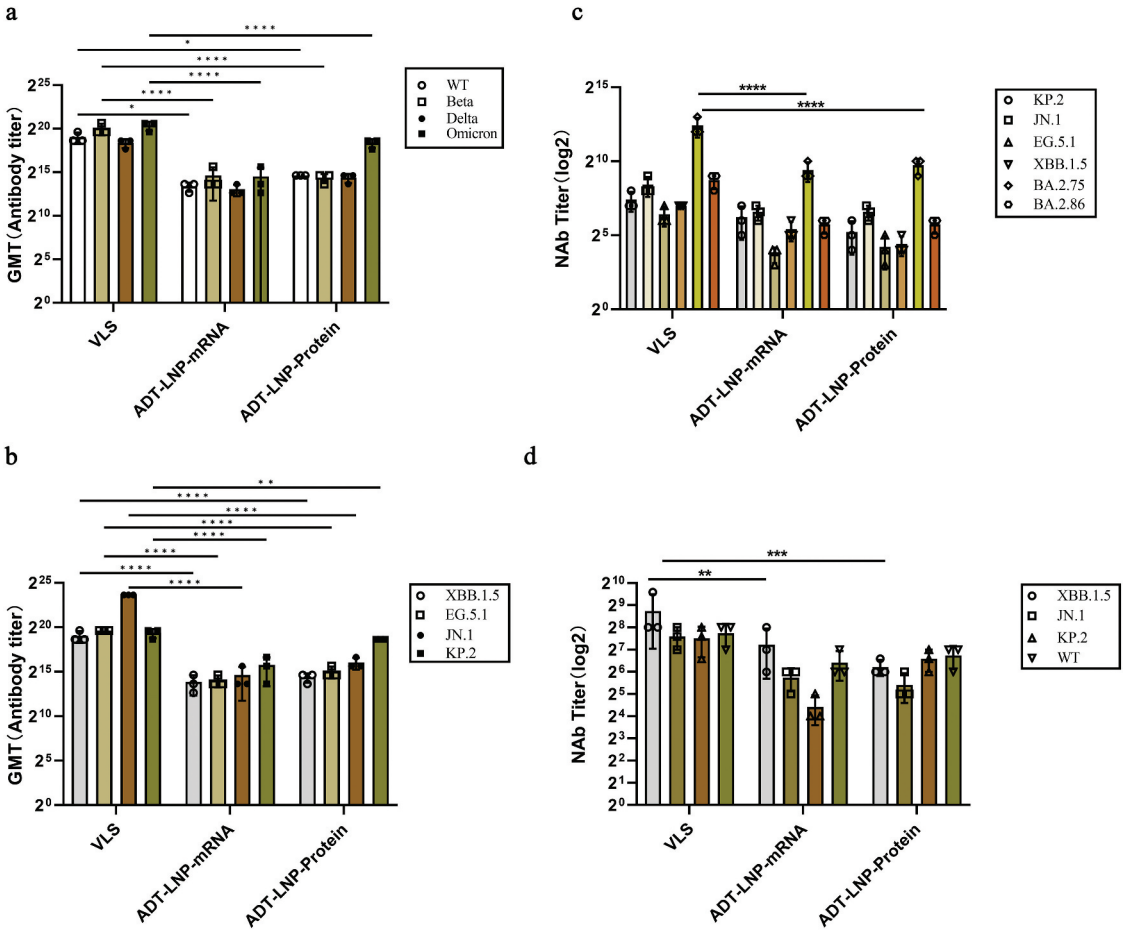

Figure 4. Adaptive immune responses were induced by VLSs in mice. SARS-CoV-2 titers of specific anti- wild-type (WT), Beta, Delta, Omicron strain antibodies (a) and XBB.1.5, EG.5.1, JN.1 and KP.2 (b) whose production was induced by VLS, ADT-LNP-mRNA and ADT-LNP-Protein; the samples were obtained on days 28 after boost injection. Titers of neutralizing antibodies against the pseudovirus (c) and real virus XBB.1.5, JN.1, KP.2 and wild-type strains (d) whose production was induced by VLSs, ADT-LNP-mRNA and ADT-LNP-Protein. The data are shown as the means ± SEMs from three independent experiments ($n = 3$). *$P < 0.05$, **$P < 0.01$, ***$P < 0.001$, ****$P < 0.0001$.

Discussion

The development of mRNA vaccines for controlling the COVID-19 pandemic provided an extended technical space capable of supporting novel vaccine development with more innovative concepts and technical means. Through a technical improvement in the composition and structure of the lipid carrier, our VLS nano-delivery system and VLS vaccine candidate have constructed a novel virus-like vaccine structure to simulate the mode of virus infection of host cells, which enables direct delivery of mRNA into antigen-presenting cells, such as dendritic cells/macrophages, via S1 protein recognition to DC-SIGN receptors in these cells, suggesting that antigens can activate the immune system beginning with innate receptors inside these cells, followed by adaptive immunity via various immune signaling pathways. This vaccine mode could be very appropriate for use against SARS-CoV-2 variants because an enhanced immune response and an extended antigenic spectrum against the variant S protein are needed in the development of new-generation vaccines. In this case, our work to prepare a novel VLS vaccine against SARS-CoV-2 focused on the following points. First, the process of virus replication in cells can be regarded as the initial step of viral antigen-mediated activation of innate immunity (32), even if the immune interference of some virus-encoding molecules can attenuate the transduction of immune signals.[22] Our VLS vaccine against SARS-CoV-2 not only enables the activation of innate immunity in cells on the basis of the advantages of the mRNA vaccine but also has an activating effect on dendritic cells/macrophages early in the process of immunization via surface S1 protein recognition by DC-SIGN, as this protein has a signal effect on exogenous antigens. This comprehensive function led to the robust immune response observed in animal tests, especially the robust binding antibody response and neutralizing antibodies against variants of SARS-

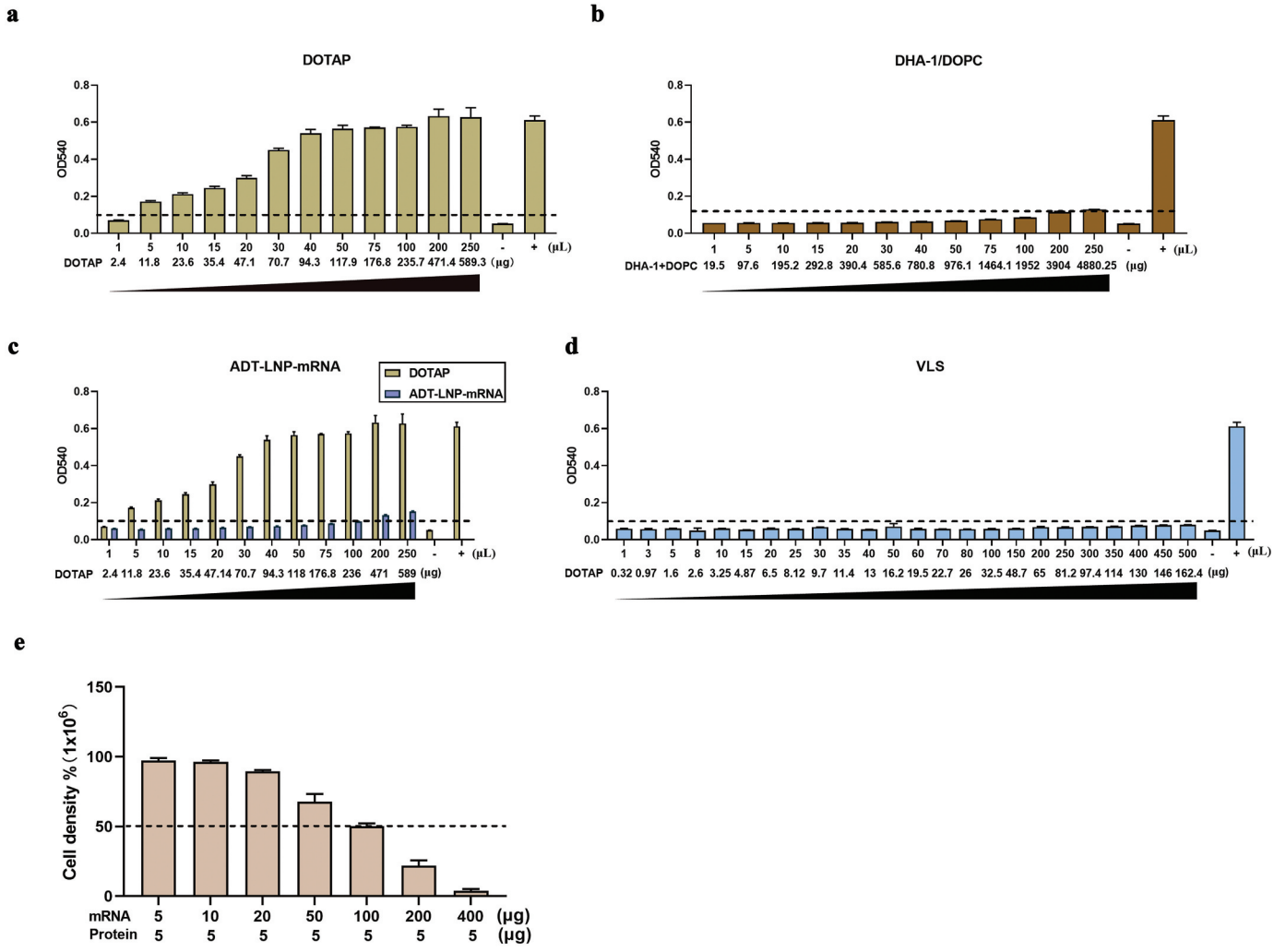

Figure 5. Safety evaluation of VLS vaccine candidates in vitro and in vivo. The hemolysis effect of DOTAP (A), DHA-1/DOPC (B), ADT-LNP-mRNA (C) and VLS (D) to treat mouse blood red cells with different dose, the abscissa represents the dose of DOTA and DHA-1/DOPC, and the ordinate represents OD540; the cytotoxicity of VLS on CCK-8 (E), the abscissa represents the dose of mRNA and protein, and the ordinate represents cell density. The data are shown as the means ± SEMs from three independent experiments ($n = 3$). * $P < 0.05$, ** $P < 0.01$, *** $P < 0.001$, **** $P < 0.0001$.

Table 6. Pathology inspection of tissues from mice immunized with the VLS vaccine.

Tissue	3 days	7 days
Muscle	±	±
Heart	–	–
Lung	–	–
Trachea	–	–
Liver	–	–
Stomach	–	–
Spleen	–	–
Spinal cord	–	–
Brain	–	–

"-" represents no symptoms, "+" represents milder symptoms, and "++" represents more obvious symptoms.

CoV-2, including most of those recently identified via ELISA, pseudovirus neutralization and real virus neutralization. Second, the immunological analysis of the VLS system suggested the possibility that a certain composition of lipid molecules could produce an artificial membrane structure with the capacity to encapsulate mRNAs and load proteins to simulate the structure and features of virus particles. This finding, that was partly published in previous paper,[11] is associated with the comprehensive technical research data presented in here implies that VLS could be used for the development of vaccines for more membranous viruses, except the vaccine against SARS-CoV-2 described here, which would be important for some viral pathogens for which vaccines are unavailable via conventional methods of development. The safety of the VLS system was investigated and analyzed in comparison with that of current mRNA vaccines. In our work, in addition to many observations according to conventional requirements for vaccine safety evaluation, the hemolysis induced probably by DOTAP and the cytotoxicity of the lipid composition were analyzed carefully. The results indicated that the safety of the VLS was within a completely acceptable range.

However, there are deficiencies in this innovative work, including the molecular mechanism of the VLS lipid system in which mRNAs are encapsulated and proteins are expressed on its surface, allowing these molecules to interact with each other and might reflect some unknown nonequilibrium thermodynamic laws that exist in basic live forms composed of

biological macromolecules. In addition, analysis of the transduction of immune signals from dendritic cells/macrophages treated with VLS vaccines to T cells is still needed for further investigation. Thirdly, the query of pre- existed antibody against S antigen blocking probably the binding of S1 protein in VLS particles to DC-SIGN receptor in dendritic cells needs identity, even if our previous work suggested the rates of VLS binding to dendritic cells in local tissues in mice immunized by inactivated SARS-CoV-2 vaccine and naive mice with no difference.

Disclosure statement

No potential conflict of interest was reported by the author(s).

Funding

This work was supported by the Shandong Weigao Litong Biological Products Co., Ltd.

Notes on contributors

Kaili Ma, professor, mainly engaged in the research of pharmacology, toxicology, neurobiology, establishment of disease animal model.

Qihan Li, professor, mainly engaged in molecular biology, genetic engineering technology, viral immunology, vaccinology and other fields related research and development of viral vaccines, production technology and quality control and quality standard system establishment.

ORCID

Qihan Li http://orcid.org/0000-0002-8932-4516

Author contributions

QHL and KLM conceived and designed the study; JJZ, YML, CYM, LCW, CEL, and XWP performed the research; RY, FYZ, LPH, YRS, HBL, AW, LF, and DXG contributed reagents; ZXZ, GX, YXW, FYH, and JBS contributed materials; JJZ, LCZ, XZ, HKY, ZST, GCL, QHL, KLM and FYZ analyzed the data; and QHL and JJZ wrote the first draft. All authors contributed to the article and approved the submitted version.

Data availability statement

The raw data supporting the conclusions of this article will be made available by the authors, and further inquiries can be directed to the corresponding authors.

Ethics Statement

The animal study was reviewed and approved by the Experimental Animal Management Association of the Shandong Weigao Litong Biological Products Co., Ltd.

References

1. Guan WJ, Ni ZY, Hu Y, Liang W-H, Ou C-Q, He J-X, Liu L, Shan H, Lei C-L, Hui DSC, et al. Clinical characteristics of coronavirus disease 2019 in China. N Engl J Med. 2020;382(18):1708–1720. doi:10.1056/NEJMoa2002032.
2. Tang P, Hasan MR, Chemaitelly H, Yassine HM, Benslimane FM, Al Khatib HA, AlMukdad S, Coyle P, Ayoub HH, Al Kanaani Z, et al. BNT162b2 and mRNA-1273 COVID-19 vaccine effectiveness against the SARS-CoV-2 delta variant in Qatar. Nat Med. 2021;27(12):2136–2143. doi:10.1038/s41591-021-01583-4.
3. Sahin U, Muik A, Derhovanessian E, Vogler I, Kranz LM, Vormehr M, Baum A, Pascal K, Quandt J, Maurus D, et al. COVID-19 vaccine BNT162b1 elicits human antibody and TH1 T cell responses. Nature. 2020;586(7830):594–599. doi:10.1038/s41586-020-2814-7.
4. Reichmuth AM, Oberli MA, Jaklenec A, Langer R, Blankschtein D. mRNA vaccine delivery using lipid nanoparticles. Ther Deliv. 2016;7(5):319–334. doi:10.4155/tde-2016-0006.
5. Karam M, Daoud G. mRNA vaccines: past, present, future. Asian J Pharm Sci. 2022;17(4):491–522. doi:10.1016/j.ajps.2022.05.003.
6. Nakagawa K, Lokugamage KG, Makino S. Viral and cellular mRNA translation in coronavirus-infected cells. Adv Virus Res. 2016;96:165–192. doi:10.1016/bs.aivir.2016.08.001.
7. Zhao Y, Qin W, Zhang JP, Hu Z-Y, Tong J-W, Ding C-B, Peng Z-G, Zhao L-X, Song D-Q, Jiang J-D, et al. HCV ires-mediated core expression in zebrafish. PLOS ONE. 2013;8(3):e56985. doi:10.1371/journal.pone.0056985.
8. Tenchov R, Bird R, Curtze AE, Zhou Q. Lipid nanoparticles─from liposomes to mRNA vaccine delivery, a landscape of research diversity and advancement. ACS Nano. 2021;15(11):16982–17015. doi:10.1021/acsnano.1c04996.
9. Chemaitelly H, Yassine HM, Benslimane FM, Al Khatib HA, Tang P, Hasan MR, Malek JA, Coyle P, Ayoub HH, Al Kanaani Z, et al. mRNA-1273 COVID-19 vaccine effectiveness against the B.1.1.7 and B.1.351 variants and severe COVID-19 disease in Qatar. Nat Med. 2021;27(9):1614–1621. doi:10.1038/s41591-021-01446-y.
10. Rahimi F, Darvishi M, Bezmin Abadi AT. 'The end' – or is it? Emergence of SARS-CoV-2 EG.5 and BA.2.86 subvariants. Future Virol. 2023;18(13):823–825. doi:10.2217/fvl-2023-0150.
11. Zhang J, Li Y, Zeng F, Mu C, Liu C, Wang L, Peng X, He L, Su Y, Li H, et al. Virus-like structures for combination antigen protein mRNA vaccination. Nat Nanotechnol. 2024;19(8):1224–1233. doi:10.1038/s41565-024-01679-1.
12. Hoffmann M, Kleine-Weber H, Schroeder S, Krüger N, Herrler T, Erichsen S, Schiergens TS, Herrler G, Wu N-H, Nitsche A, et al. SARS-CoV-2 cell entry depends on ACE2 and TMPRSS2 and is blocked by a clinically proven protease inhibitor. Cell. 2020;181(2):271–80.e8. doi:10.1016/j.cell.2020.02.052.
13. Marzi A, Gramberg T, Simmons G, Möller P, Rennekamp AJ, Krumbiegel M, Geier M, Eisemann J, Turza N, Saunier B, et al. DC-SIGN and DC-SIGNR interact with the glycoprotein of Marburg virus and the S protein of severe acute respiratory syndrome coronavirus. J Virol. 2004;78(21):12090–12095. doi:10.1128/jvi.78.21.12090-12095.2004.
14. Malone RW, Felgner PL, Verma IM. Cationic liposome-mediated RNA transfection. Proc Natl Acad Sci USA. 1989;86(16):6077–6081. doi:10.1073/pnas.86.16.6077.
15. Fan YN, Li M, Luo YL, Chen Q, Wang L, Zhang H-B, Shen S, Gu Z, Wang J. Cationic lipid-assisted nanoparticles for delivery of mRNA cancer vaccine. Biomater Sci. 2018;6(11):3009–3018. doi:10.1039/c8bm00908b.
16. Yanez Arteta M, Kjellman T, Bartesaghi S, Wallin S, Wu X, Kvist AJ, Dabkowska A, Székely N, Radulescu A, Bergenholtz J, et al. Successful reprogramming of cellular protein production through mRNA delivered by functionalized lipid nanoparticles. Proc Natl Acad Sci USA. 2018;115(15):E3351–e60. doi:10.1073/pnas.1720542115.
17. Zhang J, Wang Z, Min J, Zhang X, Su R, Wang Y, Qi W. Self-assembly of peptide–lipid nanoparticles for the efficient delivery of nucleic acids. Langmuir. 2023;39(21):7484–7494. doi:10.1021/acs.langmuir.3c00834.

18. Raman R, Patel KJ, Ranjan K. COVID-19: unmasking emerging SARS-CoV-2 variants, vaccines and therapeutic strategies. Biomolecules. 2021;11(7):993. doi:10.3390/biom11070993.
19. Tseng HF, Ackerson BK, Luo Y, Sy LS, Talarico CA, Tian Y, Bruxvoort KJ, Tubert JE, Florea A, Ku JH, et al. Effectiveness of mRNA-1273 against SARS-CoV-2 omicron and delta variants. Nat Med. 2022;28(5):1063–1071. doi:10.1038/s41591-022-01753-y.
20. Jackson LA, Anderson EJ, Rouphael NG, Roberts PC, Makhene M, Coler RN, McCullough MP, Chappell JD, Denison MR, Stevens LJ, et al. An mRNA vaccine against SARS-CoV-2 — preliminary report. N Engl J Med. 2020;383(20):1920–1931. doi:10.1056/NEJMoa2022483.
21. Regelin AE, Fankhaenel S, Gürtesch L, Regelin AE, Fankhaenel S, Gürtesch L, Prinz C, von Kiedrowski G, Massing U. Biophysical and lipofection studies of DOTAP analogs. Biochim Biophys Acta. 2000;1464(1):151–164. doi:10.1016/s0005-2736(00)00126-7.
22. Baxter D. Active and passive immunity, vaccine types, excipients and licensing. Occup Med (Lond). 2007;57(8):552–556. doi:10.1093/occmed/kqm110.